Non-thermal plasma inhibits tumor growth and proliferation and enhances the sensitivity to radiation *in vitro* and *in vivo*

LIN LIN[1*], LILI WANG[1*], YANDONG LIU[1], CHAO XU[1], YU TU[2] and JUYING ZHOU[1]

[1]Department of Radiation Oncology, The First Affiliated Hospital of Soochow University, Suzhou, Jiangsu 215006;
[2]School of Radiation Medicine and Protection, Medical College of Soochow University, Suzhou, Jiangsu 215123, P.R. China

Abstract. Cancer is a major disease currently endangering the entire world population. Morbidity and mortality have increased substantially during recent decades. Radiotherapy is a primary treatment for malignant tumors, however side-effects and tumor cell resistance to ionizing radiation reduce the efficacy of radiotherapy. In recent years, non-thermal plasma (NTP) technology been used to treat cancer. In this study, we investigated the toxic effects of NTP on normal cells and tumor cells. We explored the inhibitory effect of NTP on tumor cell proliferation and evaluated the radiation-sensitizing effects of NTP on tumor cells and its mechanisms. In short, we examined the effect of NTP-combined radiation on proliferation, the cell cycle, apoptosis and DNA damage in normal and cancer cells. We found that NTP inhibited proliferation and induced apoptosis in tumor cells. NTP was more lethal to tumor cells than to normal cells. We found promising synergies of NTP with radiotherapy on cancer cells owing to their combined cytotoxic effects by generating ROS, inducing cell cycle arrest and apoptosis. NTP may be a new candidate for the treatment of cancer.

Introduction

Cancer has emerged as a leading threat to human health worldwide (1). Radiation therapy is a primary treatment for malignant tumors; it can be administered as monotherapy or can be combined with surgery, chemotherapy, or other therapies. Ionizing radiation causes cytotoxicity through the generation of reactive oxygen species (ROS). Excessive oxidative stress causes DNA double-strand breaks (DSB), activating the DNA-damage response (DDR) system (2-4), inducing DNA damage repair, cell cycle arrest and cellular protein damage. In the process, the damage inhibits metabolic activity and causes mitochondrial malfunction in cancer cells, eventually leading to cell death (5). Tumor cells are thought to generate more ROS than their normal counterparts. Therefore, compared with normal mammalian cell lines, cancer cell lines are more sensitive to the oxidative stress induced by radiotherapy (6,7). However, the sensitivity of various cancer cells limits the use of radiation therapy. Thus, selectivity to efficient killing of cancer cells without adverse toxicity to normal cells is one of the most important therapeutic considerations in assessing new cancer therapeutic strategies.

Non-thermal plasma (NTP) generated at room temperature is a gas mixture composed of ions, electron, photons and free radicals at any desired location and intensity (8). It produces large amounts of short- and long-lived molecules including oxygen, such as ozone (O_3), superoxide anion (O_2^-), hydrogen peroxide (H_2O_2), hydroxyl radicals (HO·) and other generating-ROS species (5), depending on the concentration of the active species in the medium by generating extracellular ROS (9). Recently, NTP technology has been applied in many scientific and technological fields, including blood coagulation (10,11), promotion of wound healing (12,13) and sterilization of tissues and devices (14). It is worth emphasizing that NTP as a potential therapy for cancer has been attracting more attention by oncologists. Many studies have revealed that plasma effectively kills many types of cancer cells primarily via oxidative damage resulting in cytotoxicity both *in vitro* and *in vivo* (15-19). Another study also revealed the lower harmful effects on normal tissues than in tumors in an *in vivo* model at appropriate dosages (20). In addition, recent studies have indicated that NTP combined with conventional chemoradiotherapy or precise targeting could represent promising treatments for cancer (5,21,22).

In the present study, we evaluated whether the combination of NTP with radiotherapy was a viable approach both *in vitro* and *in vivo*. We also investigated the molecular

Correspondence to: Professor Yu Tu, School of Radiation Medicine and Protection, Medical College of Soochow University, 199 Renai Road, Suzhou Industrial Park, Suzhou, Jiangsu 215123, P.R. China
E-mail: tuyu@suda.edu.cn

Professor Juying Zhou, Department of Radiation Oncology, The First Affiliated Hospital of Soochow University, 188 Shizi Street, Suzhou, Jiangsu 215006, P.R. China
E-mail: zhoujuyingsy@163.com

*Contributed equally

anticancer mechanisms. To this end, we examined the effect of NTP-combined radiation on the proliferation, the cell cycle, apoptosis and DNA damage of normal and cancer cells. We found a promising combination of NTP with radiotherapy on cancer cells owing to their synergistically cytotoxic effects by generating ROS, inducing cell cycle arrest and apoptosis.

Materials and methods

Cell culture. Three mammalian malignant tumor cell lines and one mammalian normal cell line were used in this study. A549 (human non-small cell lung cancer cells), HeLa (human cervical cancer), HepG2 (human hepatoblastoma) (23) and GM0637 (human skin fibroblasts) cell lines were kind gifts from Professor Fan Saijun, Suchow University, Jiangsu, China. The cells were cultured in high-glucose Dulbecco's modified Eagle's medium (DMEM; Hyclone; GE Healthcare Life Sciences, Logan, UT, USA) supplemented with 10% fetal bovine serum (FBS). All stock cultures were maintained in 5% CO_2 and humidified air at 37˚C.

Animals. Healthy nude male mice, weighing 250-300 g were provided by the Laboratory Animal Center of Suchow University. Six-week old nude mice were raised in large plastic cages with a maximum of six mice per cage at 40-60% humidity, 19-23˚C. The mice were maintained on a 12-h light/dark period with 12-15 air exchanges/h and were fed with food and water *ad libitum*. The nude mice were sacrificed by cervical dislocation. The animal experiments were approved by the Ethics Committee of the First Hospital Affiliated to Soochow University.

Non-thermal jet plasma. The output voltage (3 kV) and current (40 mA) waveforms have a profile with an average power of 12 W. In our previous study, the pore diameter for non-thermal plasma was 5 mm and the tube was 10 mm away from the cultured cells. The working temperature of the plasma source was in the range of 24-32˚C at the time of treatment. The plasma plume filled with mixed gas with argon and oxygen had a length of 15 mm.

Ionizing radiation. X-radiation was delivered by a 6 MV linear accelerator (Primus, Siemens, Germany) at a dose rate of 2 Gy/min with a source-to-target distance of 1 m. For tumor irradiation, animals were anesthetized with isoflurane and positioned to place the tumor in the center of 1.0x1.0 cm radiation field, with the remainder of the animal shielded from radiation.

Cell proliferation assay. After seeding the cells in 96-well plates at a density of $5x10^3$ cells/well, the effect of irradiation and/or NTP treatment on cell viability was analyzed 24 h after treatment using an assay based on the conversion of 3-(4,5-dimethylthiazol-2-yl)-2,5-diphenyl-tetrazolium bromide (MTT; Sigma Aldrich; Merck KGaA, Darmstadt, Germany). Briefly, after the addition of MTT solution to the cell suspension (40 μl) for 4 h, the remnant formazan product was dissolved in 100 μl of DMSO. The optical density of each well was measured using a microplate reader (Bio-Tek, Winooski, VT, USA) at 540 nm. The results were presented as percentages relative to control cells.

Colony formation assay. Exponentially growing cells were trypsinized as a single cell suspension, diluted serially to appropriate densities and seeded in triplicate in six-well plates. After cell adhesion, they were treated with plasma (20 sec) for 24 h, and then subjected to 0, 2, 4, 6 or 8 Gy X-rays. The cells were then washed with PBS, cultured in drug-free medium for 14 days, fixed with methanol, and stained with Giemsa. Only colonies containing >50 cells were scored. The surviving fraction (SF) of each irradiation group was corrected by the plating efficiency (PE) of the non-irradiated control. The cell survival curves were fitted according to a multi-target single-hit model and the survival enhancement ratio (SER) was calculated as the ratio of the mean inactivation dose in control cells divided by the mean inactivation dose in plasma-treated cells. The experiment was performed in triplicate.

Immunofluorescence staining. Immunofluorescence detection of phospho-H2AX foci was performed to monitor formation of DNA double-strand breaks (DSBs). Cells cultured on coverslips were treated with plasma for 20 sec and were irradiated with a dose of 4 Gy to assure a discrimination of individual nuclear foci in immunofluorescence staining. At indicated time-points, the cells were fixed with 4% paraformaldehyde for 20 min at room temperature and were permeabilized with 0.1% Triton X-100 for 10 min at 4˚C. After blocking with Immunol Staining Blocking Buffer (Beyotime Institute of Biotechnology, Shanghai, China) for 1 h at room temperature, the cells were incubated with antibody for phospho-H2AX (Ser139) (1:1,000 dilution; cat. no. ab2893; Abcam, Cambridge Science Park, Cambridge, UK) at 4˚C overnight, followed by staining with fluorescein (FITC)-conjugated rabbit anti-mouse IgG (10 μg/ml dilution; cat. no. 315-005-045; Jackson ImmunoResearch, West Grove, PA, USA) for 1.5 h at room temperature. Finally, the samples were counterstained with 2 μg/ml DAPI and mounted in 3 μl of mounting medium (Beyotime Institute of Biotechnology). Three random fields each containing 50 cells were examined at a magnification of x100 under a Zeiss LSM5 confocal laser-scanning microscope (CarlZeiss, Jena, Germany). Nuclei containing ≥10 immunoreactive foci were scored as positive for γ-H2AX.

Flow cytometry for cell cycle detection. HeLa and HepG2 cells were harvested after 24-h treatment with non-thermal plasma (20 sec) and/or 4 Gy X-rays, respectively. After washing with ice-cold PBS, the cells were fixed with ice-cold 70% ethanol and stored at -20˚C for 1 h. Before analysis by flow cytometry, the cells were washed with PBS, resuspended in a staining solution containing 20 μl RNase A solution and 400 μl propidium iodide staining solution (Beyotime Institute of Biotechnology). Then, cell cycle distribution assessment was performed using a fluorescence-activated cell sorter (BD FACSCalibur, BD Biosciences, Franklin Lakes, NJ, USA).

Western blot analysis. Cells were harvested and homogenized in RIPA lysis buffer (cat. no. P0013C; Beyotime Institute of Biotechnology) and centrifuged at 14,000 x g for 20 min at 4˚C. Protein concentrations of the supernatants were determined
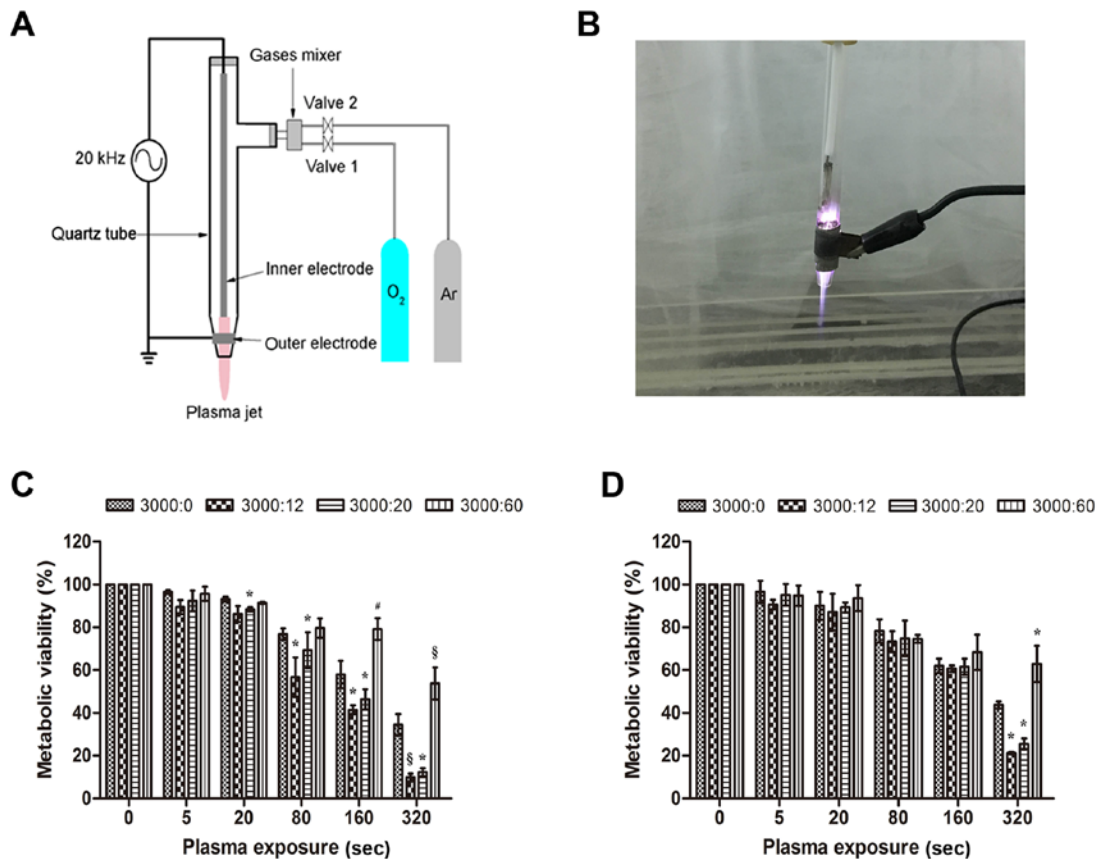
Figure 1. Plasma device and experimental setup. (A) Image of the home-made NTP jet system. (B) Schematic illustration of the NTP jet used in this study. Metabolic viability of (C) HeLa (cancer cells) and (D) GM0637 cells (normal cells) treated by NTP with different Ar/O$_2$ ratios. The results were calculated as the percentage of viable cells and presented as the mean ± SD (n=3). Compared to pure Ar-group, the significance was indicated as *P<0.05, §P<0.01, #P<0.001. NTP, non-thermal plasma.

using a BCA Protein Quantification Kit (Vazyme Biotech Co., Ltd., Nanjing, China). Western blot analysis was performed by first loading 60 μg of protein per lane which was separated using by SDS-PAGE on a 7% gel. Then the proteins were transferred to polyvinylidene difluoride membranes, and then blocked for 15 min at room temperature using QuickBlock Blocking Buffer (cat. no. P0252; Beyotime Institute of Biotechnology). The membranes were then incubated for 16 h at 4˚C using mouse polyclonal antibodies to human cyclin B1 (1:1,000 dilution; cat. no. sc-245), Cdc2 (1:1,000 dilution, cat. no. sc-53219) and phospho-Cdc2 (1:1,000 dilution, cat. no. sc-12340-R; all from Santa Cruz Biotechnology, Inc., Santa Cruz, CA, USA).

Statistical analysis. All data were expressed as the mean ± standard deviation (SD). All statistical significances were evaluated by one-way ANOVA among multiple groups, and LSD-t test between two groups, using SPSS statistics 17.0 software (SPSS, Inc., Chicago, IL, USA). A P-value <0.05 was considered to indicate a statistically significant difference.

Results

Plasma device and experimental setup. Fig. 1A displays a schematic illustration of the NTP jet used in this study. The instrument consisted of four parts: a quartz tube, two electrodes, a gas mixer and a funnel-shaped nozzle. The output voltage (3 kV) and current (40 mA) waveforms had a profile

with an average power of 12 W. In our previous study, the pore diameter for NTP was 5 mm and the tube was 10 mm from the cultured cells. The working temperature of the NTP source was 24-32˚C at the time of treatment. An image of the NTP jet is displayed in Fig. 1B. The NTP plume filled with pure argon had a length of 15 mm.

Ionizing radiation combination with NTP inhibits the proliferation of malignant tumor cells and normal cells. In order to select a suitable Ar/O$_2$ gas flow ratio, the MTT assay was used to measure the metabolic viability of HeLa (cancer cells) (Fig. 1C) and GM0637 (normal cells) (Fig. 1D) treated by NTP with various Ar/O$_2$ ratios. A pure Ar-group with a flow rate 3 l/min was used as a reference to exclude the gas effects of NTP. It was found that after 24 h of incubation, mixed gases where argon had a flow rate of 3 l/min and oxygen had a flow rate of 20 ml/min (3000:20) decreased the metabolic viability of HeLa cells by 4.8% (P<0.05), 7.5% (P<0.05), 11.6% (P<0.05) and 22.0% (P<0.05) at 20, 80, 160 and 320 sec, respectively, compared to the metabolic viability of the pure Ar-group. Using a working gas with the flow rate of 3000:12, a substantial decrease in viability was noted, 6.9% (P>0.05), 20.0% (P<0.05), 16.5% (P<0.05) and 24.6% (P<0.001) for 20, 80, 160 and 320 sec, respectively, compared to viability of the Ar-group. When the Ar/O$_2$ gas flow ratio was 3000:60, there was surprisingly less suppression after treatment for 160 sec (P<0.01) and 320 sec (P<0.001) than for
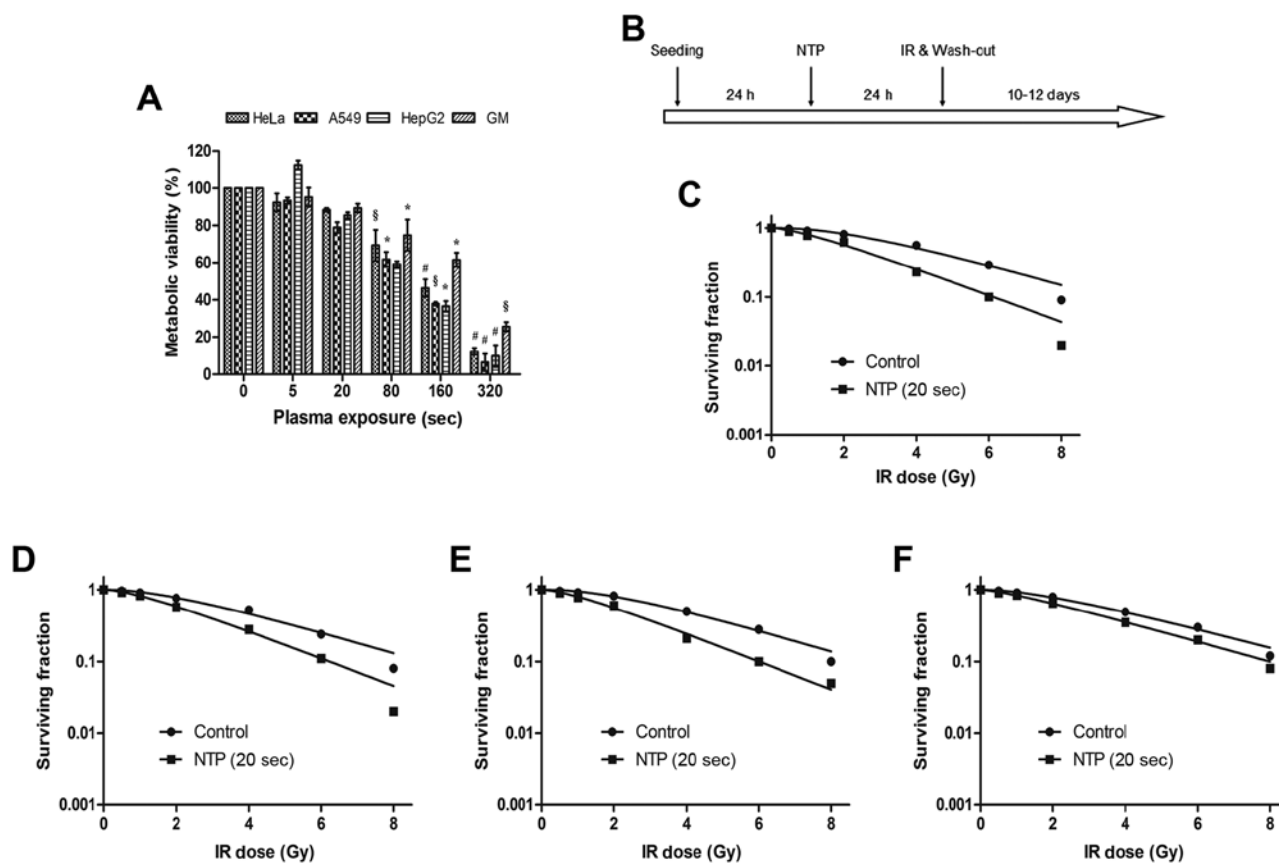
Figure 2. Ionizing radiation combination with NTP inhibits the proliferation of the malignant tumor cells and normal cells. (A) HeLa, A549, HepG2 and GM0637 cells were treated by increasing exposure time to NTP alone. Cell viability was assessed at 24 h after treatment. The Ar/O$_2$ ratio of NTP was 3000:20. The results were calculated as the percentage of viable cells and presented as the mean ± SD (n=3). Compared to control, the significance was indicated as *P<0.05, §P<0.01, #P<0.001. (B) The schematic diagram represented the proposed experimental plan to treat the cancer and normal cells using plasma and radiation. Colony formation assays were performed, and these cells were exposed to NTP for 20 sec, and to different doses of ionizing radiation. After 10 days colonies were counted and plotted as the percent survival fraction for (C) HeLa, (D) A549, (E) HepG2 and (F) GM0637 cells. The data are expressed as the mean of three independent experiments and the error bars indicate ± SD. NTP, non-thermal plasma.

the pure Ar-group at the same time. However, for the GM0637 cells, we found no significant inhibition in all four groups (P>0.05) until exposures of 320 sec, at which time there was a similar effect as observed in HeLa cells (P<0.05). Our data indicated that the inhibitory effect of NTP on tumor cells such as HeLa was more substantial than the effect on normal cells such as GM0637. We also observed that a mixed gas exhibited an inhibitory effect on the growth of HeLa cells in an exposure time-dependent manner compared to the control group.

Next, we evaluated the toxic effects of NTP on four malignant tumor cell lines (HeLa, A549, HepG2 and GM0637 cells) after 24 h of incubation with NTP at increasing time-points (Fig. 2A). The IC$_{50}$ values of plasma on HeLa, A549, HepG2 and GM0637 cell lines were 166, 144, 155 and 208 sec, respectively. All malignant tumor cells exhibited a significant decrease (P<0.05) at 80, 160 and 320 sec compared with the control group, and not surprisingly, we also observed a much lower inhibitory effect on the GM0637 cells (P<0.05). The sub-toxic time of NTP (20 sec) was adopted to investigate cancer cell proliferation inhibition by NTP combined with radiotherapy or alone.

A colony formation assay was used to detect the radiosensitivity of NTP to various cells (Fig. 2B). We found that NTP promoted radiation-induced clonogenic malignant tumor cell

death in a dose-dependent manner. When the treatment time of NTP reached 20 sec, the sensitization enhancement ratios (SERs) of HeLa (Fig. 2C), A549 (Fig. 2D), HepG2 (Fig. 2E) and GM0637 (Fig. 2F) cells were 1.29, 1.30, 1.28 and 1.03, respectively. These data indicated that NTP substantially enhanced malignant tumor cell death in three irradiated malignant tumor cell lines, while in normal cells (GM0637 cells) there was a weak difference in cell death between the irradiated group and the combination treatment group. In other words, NTP combined with ionizing radiation significantly inhibited the proliferation of tumor cells more than that of normal cells.

NTP enhances radiation-induced DNA damage in malignant tumor cells. In order to understand the effect of NTP on cell DNA damage, we detected γ-H2AX foci in HeLa and HepG2 cells by immunofluorescence with four groups including control, NTP, IR and NTP+IR groups. As displayed in Fig. 3A, NTP (20 sec) and irradiation (4 Gy) both produced γ-H2AX signals at 2 to 24 h after treatment. A peak was observed at 6 h, leading to a substantial increase in γ-H2AX staining in the NTP (56.3±7.8%, P<0.001), IR (77.0±10.4%, P<0.001) and NTP+IR groups (84.0±3.6%, P<0.001). In addition, NTP+IR resulted in a significant prolongation of γ-H2AX signals at 12 h

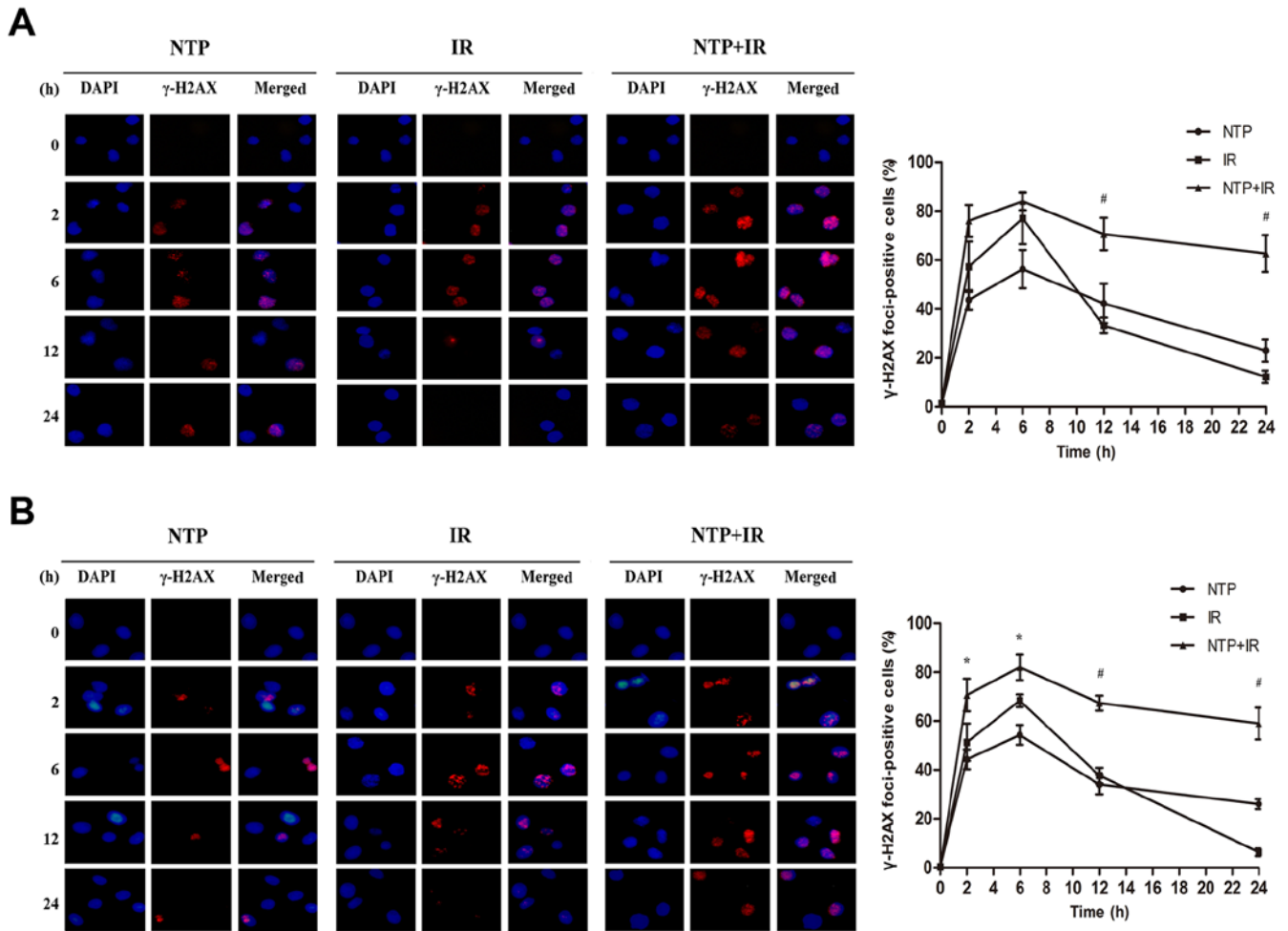Figure 3. NTP enhances radiation-induced DNA damage in malignant tumor cells. Compared to IR-treated group, NTP led to a significant increase in γ-H2AX staining in (A) HeLa cells and (B) HepG2 cells. The cells were treated with 20 sec of plasma and then exposed to 4 Gy of X-rays. At the indicated time-points, the cells were fixed for immunofluorescence detection of γ-H2AX (red) foci. Scale bar, 10 μm. Data were expressed as the percentage of cells staining positive for foci and plotted as the mean SEM of 3 independent experiments. Nuclei staining ≥10 immunoreactive foci were scored as positive for γ-H2AX. At least 100 nuclei were counted for each experiment. The significance was indicated as *P<0.05, #P<0.001, as compared to the IR-treated group. NTP, non-thermal plasma.

(70.7±6.7%) and 24 h (62.7±7.5%) compared with the IR group (33.3±3.2 and 12.3±2.5%, respectively) in HeLa cells (P<0.001 and P<0.001, respectively). We also assessed γ-H2AX foci in HepG2 cells (Fig. 3B). Similarly, a peak at 6 h was found, exhibiting a maximum number of γ-H2AX foci-positive cells in the NTP (54.3±4.0%, P<0.001), IR (68.3±2.5%, P<0.001) and NTP+IR groups (82.0±5.3%, P<0.001). Concurrently, a significant prolongation of γ-H2AX signals was observed at 12 (67.3±3.1%) and 24 h (59.0±6.6%) compared with the IR group (37.6±3.2, 6.3±1.5% respectively) in HepG2 cells (P<0.001, P<0.001 respectively). These results indicated that NTP significantly inhibited the repair of DSBs manifesting as the persistence of γ-H2AX foci at 2 to 24 h after treatment compared with irradiation alone.

NTP induces G2/M phase arrest and modulates cell cycle regulatory proteins in malignant tumor cells. To explore the effect of NTP combined with radiation on cell cycle arrest, the cell cycle distribution of HeLa and HepG2 cells were examined by flow cytometry at 24 h after treatment, and the HeLa and HepG2 cells were exposed to 20 sec of NTP and 4 Gy of

radiation. As shown in Fig. 4A and B the distribution of cell cycle phases in both cell lines after 24 h of treatment with IR, NTP and IR+NTP was revealed. It is important to point out that both NTP and ionizing radiation induced G_2/M phase arrest alone, and the combination significantly increased cell cycle arrest. These cells were arrested in the G_2/M phase of the cell cycle induced by irradiation alone (34.5±1.8%, P<0.001 for HeLa and 35.1±1.6%, P<0.001 for HepG2 cells). With the addition of a 20-sec exposure to NTP, accumulation at G_2/M was enhanced by 18.1±4.9% (P<0.01) and 9.2±2.7% (P<0.01) for HeLa and HepG2 cells, respectively. G_2/M arrest in cells treated by NTP alone ranged from 7.9 to 15.7%, (P<0.01) for HeLa and from 10.4 to 19.3%, (P<0.01) for HepG2 cells. These data indicated that NTP impacted the progression of malignant tumor cells from the G_2 to M phase.

To further explore the possible mechanisms underlying NTP-induced cell cycle arrest at 24 and 48 h, the expression profiles of cyclin B1 and cyclin-dependent kinase 1 (Cdc2) were determined by western blotting in HeLa (Fig. 4C) and HepG2 (Fig. 4D) cells treated with 20 sec of NTP and 4 Gy of radiation. The Cdc2-cyclin B1 complex is the key enzyme
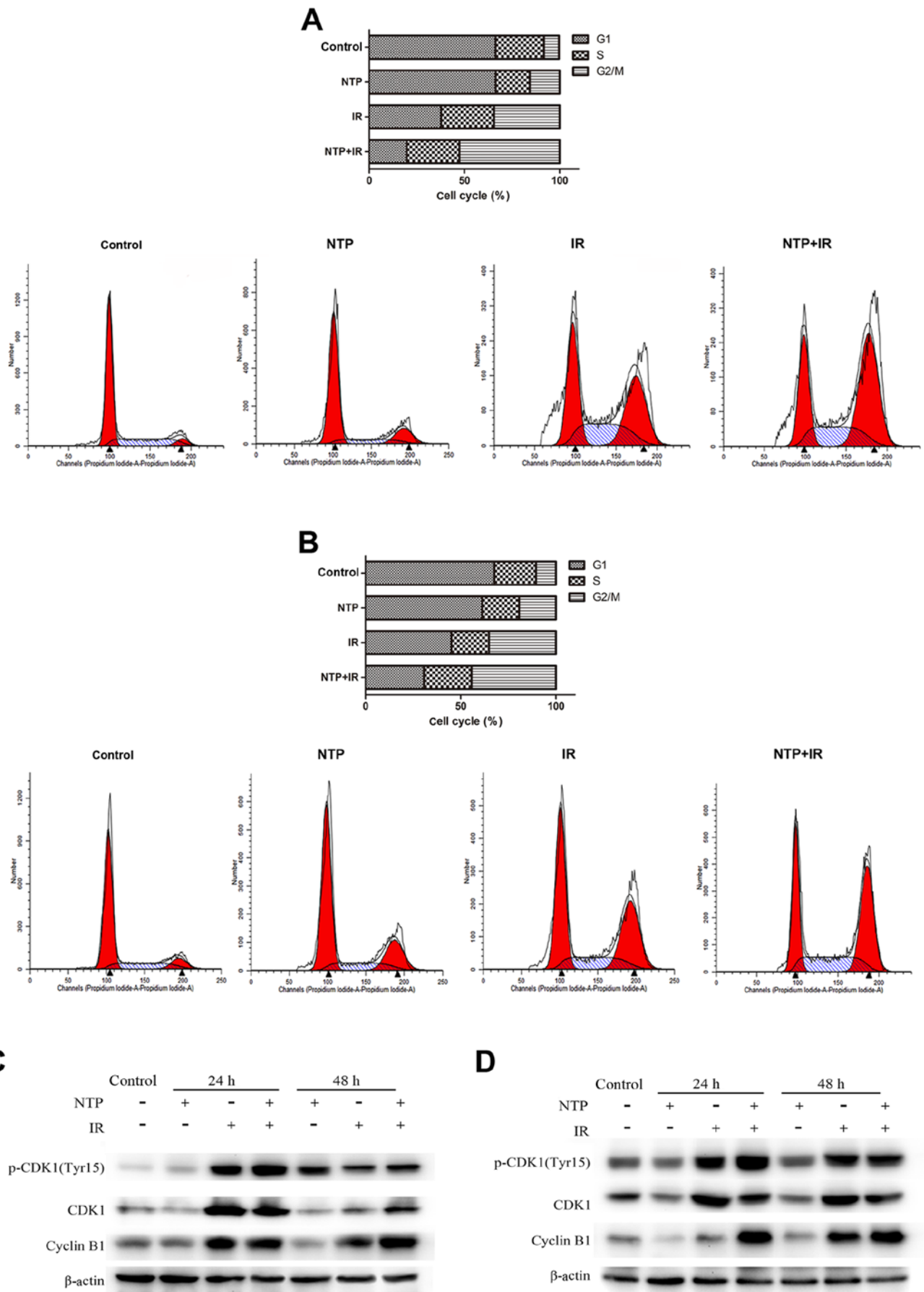
Figure 4. NTP induces G2/M phase arrest and modulates cell cycle regulatory proteins in malignant tumor cells. (A) HeLa and (B) HepG2 cells were treated with plasma, radiation or the combination modality for 24 h and then harvested for analysis of cell cycle distribution by flow cytometry. (C and D) We analyzed the expression profile of G2/M checkpoint-related proteins: Cyclin B1, Cdc2 and phospho-Cdc2 (p-Cdc2) by western blotting in the two different cell lines. The data are the representation of three independent experiments and the error bars indicate ± SD. NTP, non-thermal plasma.
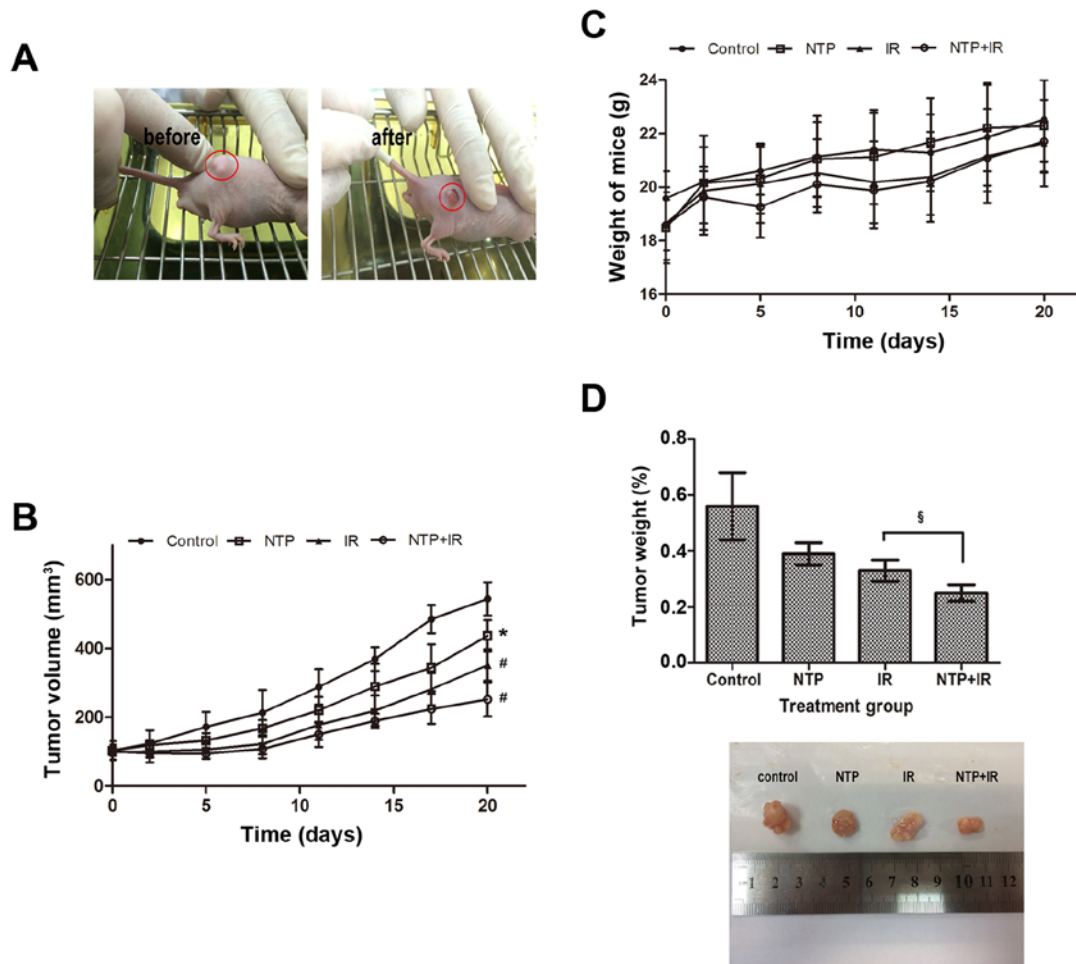
Figure 5. Ionizing radiation in combination with NTP inhibits the growth of tumors in male nude mice. When tumors reached 100 ± 30 mm³, male nude mice were randomly assigned into four groups: control, plasma (20 sec, NTP), radiation (3 Gy, IR) or the combination (NTP+IR) treatment, five mice per group. Mice in all four groups were sacrificed 20 days after treatment. (A) Typical images of mice with a single tumor before and after treatment are displayed. (B) The tumor volume was assessed at the indicated time-points after the onset of treatment on the established tumor in a murine hepatoblastoma model. The results were calculated and presented as the mean $\pm$ SD (n=5). Compared to the control, the significance was indicated as *$P<0.05$, #$P<0.001$. (C) Body weight of mice with different treatments was assessed at the indicated time-points. (D) We compared the tumor weight when the mice were sacrificed at 20 days after treatment and the images revealed the typical size of the four groups. The significance was indicated as §$P<0.01$, as compared to the IR-treated group. NTP, non-thermal plasma; NTP, non-thermal plasma.

regulating G_2 to M transition and is controlled by phosphorylation at various sites. We found that treatment with NTP alone slightly increased basal levels of phospho-Cdc2 (p-Cdc2) and cyclin B1 at 24 h, but the expression levels of the Cdc2 protein were almost not affected, compared to those of the control group. Western blot analysis revealed that combination treatment markedly increased the levels of p-Cdc2 and cyclin B1 in both cell lines at 24 h compared with those of the IR group. Concurrently, the protein levels of Cdc2 exhibited no significant differences in the IR group and NTP+IR group at 24 h. Additionally, a substantial increase of cyclin B1 was detected at 48 h, but the expression levels of Cdc2 and p-Cdc2 protein were not affected. Therefore, NTP appeared to promote radiation-induced Cdc2 phosphorylation and cyclin B1 accumulation thus regulating G_2 to M transition.

Ionizing radiation in combination with NTP inhibits the growth of tumors in male nude mice. We assessed the radio-sensitizing effects of NTP on hepatoblastoma cells *in vivo*, using male nude mice bearing HepG2 cell xenograft tumors. We examined the

skin of the mice after NTP or radiation treatment and did not observe any damage to the skin after 1-20 days of treatment. We found that tumors exhibited significant changes before and after treatment (Fig. 5A). As shown in Fig. 5B, NTP or irradiation alone produced significant tumor volume regression by day 20, reducing tumor volume by 19.7% ($P<0.05$) for NTP and 35.4% ($P<0.001$) for the IR group, compared to volume of the control group. However, the combination of plasma and radiation produced more tumor volume regression by 53.7% ($P<0.001$) for the NTP+IR group. Notably, combined treatment prolonged the time required for tumor volume doubling relative to radiation or NTP alone. However, we observed no complete regression with either treatment alone. All four treatments were well tolerated by the animals until the end of the treatment course with no evidence of local serious skin damage or systemic toxicity such as weight loss (Fig. 5C).

Tumor weight measurements performed 24 h after the end of the treatment course (Fig. 5D) revealed lower tumor weight of 30.4% ($P>0.05$) for NTP, 41.1% ($P<0.05$) for IR and 55.4% ($P<0.05$) for the NTP+ IR group, compared to the weight of the
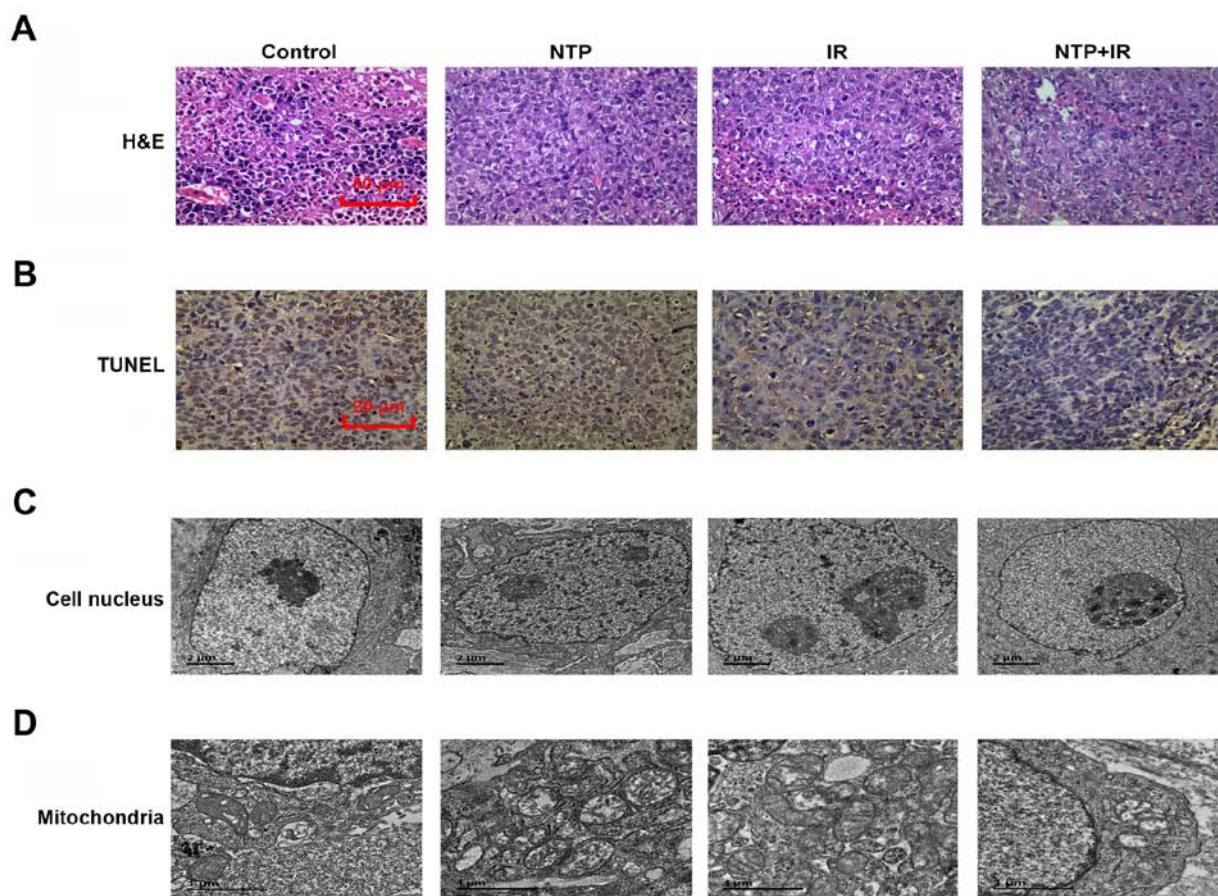
Figure 6. Ionizing radiation in combination with NTP enhanced the antitumor activity *in vivo*. (A) H&E and (B) TUNEL staining were analyzed for apoptosis in tumor sections after NTP, radiation and the combination modality at 20 days after treatment. Scale bars, 50 μm for H&E staining and 20 μm for TUNEL staining. The electron microscope was used to observe the changes of (C) the cell nucleus and (D) mitochondria in different groups after 20 days of treatment. Scale bars, 2 μm for the cell nucleus and 1 μm for mitochondria. All the results were obtained from three independent experiments. NTP, non-thermal plasma.

control group. In addition, we found a significant difference between the IR and combined treatment groups (P<0.05). The typical tumor size of these four groups also showed a similar change. This indicated that NTP enhanced radiosensitivity of hepatoblastoma cells *in vivo* without serious skin damage or systemic toxicity.

Ionizing radiation in combination with NTP enhances antitumor activity in vivo. We performed a microscopic examination using H&E staining after the end of the treatment course (20 days) (Fig. 6A). The hepatoblastoma mouse model treated with combined therapy exhibited a looser arrangement of cancer cells and larger areas of necrosis compared with cells with NTP or radiation treatment alone. As shown in Fig. 6B, TUNEL staining after the end of the treatment course (20 days) revealed that, compared to the control group, NTP or radiation treatment alone increased the number of apoptotic cells from 1.0 to 5.8% (P<0.05) or 7.5% (P<0.05), respectively. We also observed a significantly enhanced level of apoptotic cells (11.0%, P<0.05) in the combination treatment group compared to the control treatment group.

We also investigated changes in the nuclear membrane and mitochondria by electron microscope at 20 days after treatment. The nuclear membrane, which in NTP or radiation treatment alone became thicker than that of the control group, exhibited no significant destruction of its structural integrity. However, in the combination treatment group, we not only found a thicker nuclear membrane, but also cell shrinkage, nuclear chromatin condensation and fragmentation (Fig. 6C). Similar changes were observed in the structure of mitochondria of tumor tissue (Fig. 6D). Substantial numbers of swollen mitochondria were found in the plasma and radiation treatment groups. In the combined group, marked changes could be found in the tumor tissue, including formation of mitochondrial vacuoles and apoptotic bodies. Collectively, these results indicated that NTP and radiation combination treatment altered mitochondrial metabolism, inducing apoptotic cell death.

Discussion

The scheme of our NTP jet device was based on the myriad potential clinical applications of NTP, including the most important species generated by NTP, high levels of ROS for the inhibition of cancer growth (5,8,9,24). We simplified the gas mixture to oxygen and argon only. First, in order to exclude the physical effect of gas flow imposing physical shear stress on the adherent cells, we designed a set of experiments using pure argon with a flow rate of 3 l/min. Then, we selected the most suitable Ar/O$_2$ gas flow ratio. Three groups

with various mixture flow rates of oxygen were set. At oxygen flow rates of 12 and 20 ml/min, an exposure time-dependency was observed in HeLa cells, but no significant changes were observed in GM0637 cells. These results indicated that ROS generated by NTP treatment may have led to much more harm to cancer cells than to normal cells at the same doses. The distinctive cellular responses may be related to differential adhesion behavior, metabolic viability and resistance to oxidative stress between mammalian cancer cells and normal cells (5,25). Pro-apoptotic genes were upregulated and anti-apoptotic genes were downregulated concurrently by ROS such as O_3, O_2^-, H_2O_2, HO· in cancer cells, and eventually cells underwent apoptosis (5). However, treatment of mixed gas with oxygen at 60 ml/min, gave rise to even less cell death in both cell lines compared with rates in the control group. The possible explanation for the observed phenomenon is that much higher levels of ROS may activate DNA damage repair pathways and may enhance cell growth. This notion requires further study in detail.

In the present study, we revealed that NTP inhibited cell growth in an exposure time-dependent manner. Next, we observed that, at a short exposure time (20 sec), NTP enhanced radiation-induced inhibition of growth of malignant tumor cells, while there was hardly reduction of growth of normal cells. Radiosensitization by NTP in cancer cells was associated with great DNA damage as well as cell cycle arrest in the G2/M phase.

Various exogenous DNA-damaging factors, such as non-thermal plasma, ionizing radiation and a large number of chemical substances, attack DNA inducing simple DNA mutations, DNA single and double-strand breaks (SSB, DSB), or more complex changes (26,27). The cellular responses to DNA damage, collectively known as DDR, act as a biological barrier to constant exposure to DNA-damaging agents (28). DDR engages signaling pathways that regulate DNA repair pathways, as well as transit through the cell cycle and apoptosis (29). Recent studies revealed that activation of DDR prevented tumorigenesis by inducing cellular senescence or apoptosis of cancer cells (30,31). Consequently, we believe that cellular responses to DNA damage as well as cell cycle checkpoint responses are key issues in the pathogenesis of cancer. Although cellular proliferation is tightly controlled by several Cdk-cyclin complexes that control the mammalian cell cycle division (32), the genes encoding these proteins are often disrupted via alterations such as p53 mutations inducing lack of a functional G1 checkpoint, hence causing unrestrained cancer growth (33). Therefore, an attractive approach may rely on intact G2 checkpoints governed by Cdk1 (Cdc2)-cyclin B, allowing extended time to cell senescence or apoptosis prior to mitosis in response to DNA-damaging agents (28).

In support of this notion, we found that NTP combined with irradiation significantly increased persistent γ-H2AX expression in malignant tumor cells that lasted for a much longer time than was observed with irradiated cells only. The impairment of DNA could enhance apoptosis induced by combination treatment. Consistently, we demonstrated that NTP inhibited cancer cell growth and active cell senescence by inducing G2/M cell cycle arrest. It has already been well established that early events regulating cell cycle arrest in the DDR include activation of the key signaling pathways ATM/CHK2 (ataxia-telangiectasia

mutated/checkpoint kinase 2) and ATR/CHK1 (ATM and RAD3-related/checkpoint kinase 1) (34,35). Previous studies revealed that ionizing radiation induced the ATM pathway, while NTP induced the ATR pathway (36,37). Subsequently, both pathways synergistically resulted in a stable state of proliferative arrest of the G2/M phase, leading to cancer cell death (38,39). Furthermore, it is worth mentioning that the popular therapeutic targets of cancer treatment include the myriad inhibitors of cell-cycle checkpoints that disrupt radiation-induced G2/M checkpoints. Earlier studies found that abrogating G2/M arrest led to decreased repair of DNA damage that may take place before cell division, resulting in preferential malignant tumor cell death (40,41). In the present study, we highlighted the role of a low dose of non-thermal plasma that induced malignant tumor cell senescence by causing cell cycle arrest of the G2/M phase, indicating similar results with some recent studies (38,39,42).

We believe that NTP induces G2/M cell cycle blocking, however, the G2/M phase is only the most sensitive period for radiation treatment. Therefore, a small dose of NTP may constitute an effective radiotherapy sensitization. However, we speculate as to whether this kind of cell cycle arrest is lasting and irreversible, or short and reversible. If the former, NTP could represent a promising clinical outcome in that cancer cells would always stay at the G2 phase, and never proceed to mitosis. If the latter, while growth of tumor cells would be suppressed at first, there would subsequently be explosive growth, leading to disease recurrence. Clinically, this may be detrimental to long-term survival, since the recovery of self-healing may be the beginning of a recurrence of malignant tumors. Therefore, further mechanistic study is required and we will focus on this further.

Further studies of combined treatment in eligible animal models were carried out. We found that plasma combined with ionizing radiation inhibited malignant tumor growth *in vivo*. It should also be noted that the mitochondrial apoptosis pathway was activated and various morphological changes occurred, including chromatin condensation and cell blebbing. Combination treatment may induce mitochondrial ROS accumulation, resulting in excessive mitochondrial fragmentation and clustering that are now thought to act as central coordinators of cell death (43-45). However, the molecular mechanisms remain unknown and require further study.

To the best of our knowledge, this is the first study to reveal the combined effects of treatment with NTP and radiation. Collectively, our data strongly support the conclusion that combination treatment can preferentially and selectively kill malignant tumor cells *in vitro* and inhibit tumor growth *in vivo*. Additionally, we also found that combination treatment activated DDR in malignant tumor cells, allowing DNA damage and cell cycle arrest. Moreover, the mitochondrial apoptosis pathway was activated, inhibiting malignant tumor growth in an animal model. Finally, we conclude that this combination treatment may represent a novel strategy for malignant tumor therapeutics, and this study may provide some basis with which to understand its essential mechanisms.

Acknowledgements

Availability of data and materials

The datasets used during the present study are available from the corresponding author upon reasonable request.

Authors' contributions

LL designed the *in vitro* experiments, acquired, analyzed and interpreted the immunofluorescence staining, flow cytometry (for the cell cycle detection) and western blot analysis data and drafted the manuscript for these parts. LW designed the *in vivo* experiments, acquired, analyzed and interpreted the H&E staining and TUNEL staining data and drafted the manuscript for these parts. YL acquired, analyzed and interpreted the colony formation and cell proliferation assay data and drafted the manuscript for these parts. CX acquired, analyzed and interpreted the data in the creation of the hepatoblastoma mouse model and drafted manuscript for this part. YT conceived the *in vitro* experiments and critically revised the study for important intellectual content. JZ conceived the *in vivo* experiments and critically revised the study for important intellectual content. All authors read and approved the manuscript and agree to be accountable for all aspects of the research in ensuring that the accuracy or integrity of any part of the work are appropriately investigated and resolved.

Ethics approval and consent to participate

The animal experiments were approved by the Ethics Committee of the First Hospital Affiliated to Soochow University.

Patient consent for publication

Not applicable.

Competing interests

The authors declare that they have no competing interests.

References

1. Jemal A, Bray F, Center MM, Ferlay J, Ward E and Forman D: Global cancer statistics. Cancer J Clin 61: 69-90, 2011.
2. Curtin NJ: DNA repair dysregulation from cancer driver to therapeutic target. Nat Rev Cancer 12: 801-817, 2012.
3. Roos WP and Kaina B: DNA damage-induced cell death: From specific DNA lesions to the DNA damage response and apoptosis. Cancer Lett 332: 237-248, 2013.
4. Filomeni G, De Zio D and Cecconi F: Oxidative stress and autophagy: The clash between damage and metabolic needs. Cell Death Differ 22: 377-388, 2015.
5. Kaushik N, Uddin N, Sim GB, Hong YJ, Baik KY, Kim CH, Lee SJ, Kaushik NK and Choi EH: Responses of solid tumor cells in DMEM to reactive oxygen species generated by non-thermal plasma and chemically induced ROS systems. Sci Rep 5: 8587, 2015.
6. Kawagishi H and Finkel T: Unraveling the truth about antioxidants ROS and disease: Finding the right balance. Nat Med 20: 711-713, 2014.
7. Wu H, Lin J, Liu P, Huang Z, Zhao P, Jin H, Ma J and Gu N: Reactive oxygen species acts as executor in radiation enhancement and autophagy inducing by AgNPs. Biomaterials 101: 1-9, 2016.
8. Mounir L and Tamer A: Arc-free atmospheric pressure cold plasma jets: A review. Plasma Proc Polymers 4: 777-788, 2007.
9. Chen Z, Lin L, Cheng X, Gjika E and Keidar M: Treatment of gastric cancer cells with nonthermal atmospheric plasma generated in water. Biointerphases 11: e031010, 2016.
10. Ikehara S, Sakakita H, Ishikawa K, Akimoto Y, Yamaguchi T, Yamagishi M, Kim J, Ueda M, Ikeda JI, Nakanishi H, *et al*: Plasma blood coagulation without involving the activation of platelets and coagulation factors. Plasma Process Polymers 12: 1348-1353, 2015.
11. Miyamoto K, Ikehara S, Takei H, Akimoto Y, Sakakita H, Ishikawa K, Ueda M, Ikeda J, Yamagishi M, Kim J, *et al*: Red blood cell coagulation induced by low-temperature plasma treatment. Arch Biochem Biophys 605: 95-101, 2016.
12. Mitra A, Morfill GE, Shimizu T, Steffes B, Isbary G, Schmidt HU, Li YF and Zimmermann ZL: Applications in plasma medicine: A SWOT approach. Compos Inter 19: 231-238, 2012.
13. Mohd Nasir N, Lee BK, Yap SS, Thong KL and Yap SL: Cold plasma inactivation of chronic wound bacteria. Arch Biochem Biophys 605: 76-85, 2016.
14. Stryczewska HD, Jakubowski T, Kalisiak S, Giżewski T and Pawłat J: Power systems of plasma reactors for non-thermal plasma generation. J Adv Oxid Technol 16: 52-62, 2013.
15. Babington P, Rajjoub K, Canady J, Siu A, Keidar M and Sherman JH: Use of cold atmospheric plasma in the treatment of cancer. Biointerphases 10: e029403, 2015.
16. Hou J, Ma J, Yu KN, Li W, Cheng C, Bao L and Han W: Non-thermal plasma treatment altered gene expression profiling in non-small-cell lung cancer A549 cells. BMC Genomics 16: 435, 2015.
17. Weiss M, Gümbel D, Hanschmann EM, Mandelkow R, Gelbrich N, Zimmermann U, Walther R, Ekkernkamp A, Sckell A, Kramer A, *et al*: Cold atmospheric plasma treatment induces anti-proliferative effects in prostate cancer cells by redox and apoptotic signaling pathways. PLoS One 10: e0130350, 2015.
18. Mirpour S, Piroozmand S, Soleimani N, Jalali Faharani N, Ghomi H, Fotovat Eskandari H, Sharifi AM, Mirpour S, Eftekhari M and Nikkhah M: Utilizing the micron sized non-thermal atmospheric pressure plasma inside the animal body for the tumor treatment application. Sci Rep 6: e29048, 2016.
19. Schmidt A, *et al*: In vitro approaches to test cold plasma technology as a new treatment option for supportive skin cancer therapy. Exp Dermatol 25: E35-E35, 2016.
20. Shashurin A, Keidar M, Bronnikov S, Jurjus RA and Stepp MA: Living tissue under treatment of cold plasma atmospheric jet. Appl Phys Lett 93: e181501, 2008.
21. Brullé L, Vandamme M, Riès D, Martel E, Robert E, Lerondel S, Trichet V, Richard S, Pouvesle JM and Le Pape A: Effects of a non thermal plasma treatment alone or in combination with gemcitabine in a MIA PaCa2-luc orthotopic pancreatic carcinoma model. PLoS One 7: e52653, 2012.
22. Chang JW, Kang SU, Shin YS, Seo SJ, Kim YS, Yang SS, Lee JS, Moon E, Lee K and Kim CH: Combination of NTP with cetuximab inhibited invasion/migration of cetuximab-resistant OSCC cells: Involvement of NF-κB signaling. Sci Rep 5: 18208, 2015.
23. López-Terrada D, Cheung SW, Finegold MJ and Knowles BB: Hep G2 is a hepatoblastoma-derived cell line. Hum Pathol 40: 1512-1515, 2009.
24. Ma Y, Ha CS, Hwang SW, Lee HJ, Kim GC, Lee KW and Song K: Non-thermal atmospheric pressure plasma preferentially induces apoptosis in p53-mutated cancer cells by activating ROS stress-response pathways. PLoS One 9: e91947, 2014.
25. Gweon B, Kim M, Kim DB, Kim D, Kim H, Jung H, Shin J and Choe W: Differential responses of human liver cancer and normal cells to atmospheric pressure plasma. Appl Phys Lett 99: e063701, 2011.
26. Jackson SP and Bartek J: The DNA-damage response in human biology and disease. Nature 461: 1071-1078, 2009.
27. Lord CJ and Ashworth A: The DNA damage response and cancer therapy. Nature 481: 287-294, 2012.
28. Poehlmann A and Roessner A: Importance of DNA damage checkpoints in the pathogenesis of human cancers. Pathol Res Pract 206: 591-601, 2010.
29. Li Z, Pearlman AH and Hsieh P: DNA mismatch repair and the DNA damage response. DNA Repair (Amst) 38: 94-101, 2016.
30. Ciccia A and Elledge SJ: The DNA damage response: Making it safe to play with knives. Mol Cell 40: 179-204, 2010.

31. Bartek J, Bartkova J and Lukas J: DNA damage signalling guards against activated oncogenes and tumour progression. Oncogene 26: 7773-7779, 2007.
32. Tamura K: Development of cell-cycle checkpoint therapy for solid tumors. Jpn J Clin Oncol 45: 1097-1102, 2015.
33. Wang Z, Lai ST, Ma NY, Deng Y, Liu Y, Wei DP, Zhao JD and Jiang GL: Radiosensitization of metformin in pancreatic cancer cells via abrogating the G2 checkpoint and inhibiting DNA damage repair. Cancer Lett 369: 192-201, 2015.
34. Manic G, Obrist F, Sistigu A and Vitale I: Trial Watch: Targeting ATM-CHK2 and ATR-CHK1 pathways for anticancer therapy. Mol Cell Oncol 2: e1012976, 2015.
35. Leary A, Auguste A and Mesnage S: DNA damage response as a therapeutic target in gynecological cancers. Curr Opin Oncol 28: 404-411, 2016.
36. Chang JW, Kang SU, Shin YS, Kim KI, Seo SJ, Yang SS, Lee JS, Moon E, Baek SJ, Lee K and Kim CH: Non-thermal atmospheric pressure plasma induces apoptosis in oral cavity squamous cell carcinoma: Involvement of DNA-damage-triggering sub-G(1) arrest via the ATM/p53 pathway. Arch Biochem Biophys 545: 133-140, 2014.
37. Maréchal A and Zou L: DNA Damage Sensing by the ATM and ATR Kinases. Cold Spring Harb Perspect Biol 5: a012716, 2013.
38. Baz-Martínez M, Da Silva-Álvarez S, Rodríguez E, Guerra J, El Motiam A, Vidal A, García-Caballero T, González-Barcia M, Sánchez L, Muñoz-Fontela C, et al: Cell senescence is an anti-viral defense mechanism. Sci Rep 6: 37007, 2016.
39. Lee N, Ryu HG, Kwon JH, Kim DK, Kim SR, Wang HJ, Kim KT and Choi KY: SIRT6 depletion suppresses tumor growth by promoting cellular senescence induced by DNA damage in HCC. PLoS One 11: e0165835, 2016.
40. Pitts TM, Davis SL, Eckhardt SG and Bradshaw-Pierce EL: Targeting nuclear kinases in cancer: Development of cell cycle kinase inhibitors. Pharmacol Ther 142: 258-269, 2014.
41. Bretones G, Delgado MD and León J: Myc and cell cycle control. Biochim Biophys Acta 1849: 506-516, 2015.
42. Wang LX, Wang JD, Chen JJ, Long B, Liu LL, Tu XX, Luo Y, Hu Y, Lin DJ, Lu G, et al: Aurora A kinase inhibitor AKI603 induces cellular senescence in chronic myeloid leukemia cells harboring T315I mutation. Sci Rep 6: e35533, 2016.
43. Ruwan Kumara MH, Piao MJ, Kang KA, Ryu YS, Park JE, Shilnikova K, Jo JO, Mok YS, Shin JH, Park Y, et al: Non-thermal gas plasma-induced endoplasmic reticulum stress mediates apoptosis in human colon cancer cells. Oncol Rep 36: 2268-2274, 2016.
44. Saito K, Asai T, Fujiwara K, Sahara J, Koguchi H, Fukuda N, Suzuki-Karasaki M, Soma M and Suzuki-Karasaki Y: Tumor-selective mitochondrial network collapse induced by atmospheric gas plasma-activated medium. Oncotarget 7: 19910-19927, 2016.
45. Green DR and Reed JC: Mitochondria and apoptosis. Science 281: 1309-1312, 1998.